Contents lists available at ScienceDirect

# Applied Catalysis B: Environmental

# Silica support modifications to enhance Pd-catalyzed deoxygenation of stearic acid

Nicolás A. Grosso-Giordano [1], Todd R. Eaton [2], Zhenyu Bo, Sara Yacob [3], Chieh-Chao Yang, Justin M. Notestein[*]

*Department of Chemical and Biological Engineering, Northwestern University, Evanston, IL, United States*

### ABSTRACT

The catalytic deoxygenation of fatty acids has recently received significant attention as a low-hydrogen approach to biomass feedstock deoxygenation for production of hydrocarbon fuels with superior properties to biodiesel. Unfortunately, it is a challenging reaction to push to high yields. Of typical catalysts, Pd/C is typically reported to give the best performance, while most oxide supports are inferior, with exceptions for very specific preparation and pre-treatment protocols. Here, we investigate the role of organosilane-modified silicas as supports for the Pd-catalyzed deoxygenation of stearic acid at 300 °C under inert atmosphere. Comparing aminopropylsilane-modified, phenylsilane-modified, and unmodified silica supports with Pd incorporated by several methods, it is first shown that changes in dispersion alone do not account for improvements in deoxygenation yields. Capping silanols with phenylsilane is also ineffective on its own in improving deoxygenation yields. The most effective treatment is shown to be a co-deposition of phenylsilane and aminopropylsilane before Pd incipient wetness impregnation, followed by direct reduction of the catalyst, which gives heptadecane yields >85%, exceeding even the productivity of Pd/C. These results demonstrate that basic, aromatic-rich surfaces are accessible through organosilane grafting and that these surfaces can control Pd particle sizes and the adsorption of stearic acid and products. This work improves our understanding of support effects for biomass feedstock deoxygenation catalysts and could help design new catalysts that take advantage of modified inorganic supports.

© 2016 Elsevier B.V. All rights reserved.

## 1. Introduction

The renewable production of liquid fuels from biomass feedstocks is one approach for the replacement of fossil fuels [1]. Biodiesel produced by the transesterification of triglycerides to alkyl esters is an established method for capturing the high energy content in plant oils and animal fats; however, when compared to traditional diesel, it suffers from increased $NO_x$ exhaust emissions and poorer oxidative stability and cold flow properties. Furthermore, challenges still remain for utilizing cheaper waste oils and grease as feedstocks for biodiesel production owing to their high free fatty acid (FFA) content [2]. Biomass feedstock deoxygenation

can eliminate the fuel quality problems associated with biodiesel, and could tolerate high FFA contents. Existing infrastructure can be used in hydrodeoxygenation of these feedstocks, but crucially requires high pressures of valuable $H_2$ [2,3].

The catalytic decarboxylation of carboxylic acids has received significant research attention as a low-hydrogen approach to the production of hydrocarbons through biomass feedstock deoxygenation [4,5]. Early experiments established the decarboxylation of stearic acid to *n*-heptadecane (Scheme 1) under an inert atmosphere as a probe reaction for biomass feedstock deoxygenation [6]. Subsequent studies found that Pd was the most active metal catalyst for this reaction, and that an activated carbon support was superior relative to alumina under laboratory conditions [7]. Additional studies investigated the effect of reaction temperature [8], extended the application of the reaction to decarboxylation of unsaturated feedstocks [9] and fatty acid derivatives [10], and also found that catalyst deactivation occurred quickly and irreversibly [11]. Other researchers focused on detailing the reaction mechanism [12,13] and studying the nature of the catalyst deactivation, finding that $H_2$-deficient atmospheres result in more severe deacti-

---
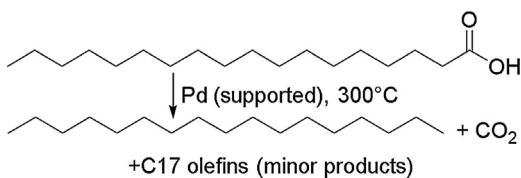
**Scheme 1.** Deoxygenation of stearic acid by decarboxylation to (primarily) *n*-heptadecane.

vation [14–16], as can be expected. Additionally, some researchers found that intermediate Pd dispersions resulted in better activity due to low active site availability at low dispersions and an undesired influence of the activated carbon on the metal at very high dispersions [17].

While these prior studies used Pd/C with excellent outcomes, other researchers found that using inorganic supports results in inferior activity. In the case of alumina supports, the catalyst deactivates very quickly, and when using silica, the reaction proceeds via decarbonylation instead of decarboxylation [18]. Others, however, have succeeded in supporting Pd on mesoporous silica with excellent results for decarboxylation in both $H_2$-containing [19] and inert [20] atmospheres. In parallel, the role of activated carbon supports has been further investigated. It has been found that (1) more alkaline activated carbon supports increase selectivity to *n*-heptadecane in the deoxygenation of stearic acid [7] and ethyl stearate [10], (2) a Sibunit carbon forms *n*-pentadecane [8], and (3) increased polarity of a carbon nanofiber support increases catalyst activity [21]. These studies make it clear that the support strongly influences catalyst performance in ways that are not entirely understood or controlled.

To further investigate synthetic handles on stearic acid deoxygenation catalysts, we studied the effect of Pd incorporation method (deposition, incipient wetness impregnation or strong electrostatic adsorption [22]) and silica modifications with phenyl- and aminopropylsilanes to separate effects of Pd dispersion and support chemistry on the ultimate deoxygenation yield and selectivity. Accounting for differences in Pd dispersion, we demonstrate significant intrinsic support effects that are tunable by synthesis and which may prove useful in formulating improved catalysts for biomass feedstock deoxygenation.

## 2. Experimental methods

### 2.1. General considerations

Solvents, unless otherwise specified, were ACS grade or higher and used without purification. Toluene was distilled over $CaH_2$ before use. Water was purified using a Barnstead model D11901 water purification system to 18 MΩ-cm resistivity. Silica ($SiO_2$) was nonporous Aeroperl fumed $SiO_2$ (Evonik-Degussa, 340 m$^2$/g surface area, mechanically compacted 7 nm primary particles). A non-porous silica was chosen to help minimize limitations from internal diffusion or pore collapse/plugging under reaction conditions. Synthesis and reaction solvents were used as received or treated as noted in the text. Scheme 2 gives a general scheme of catalysts synthesized.

### 2.2. 3-Aminopropylsilane-modified silica (**A**)

Silica (13 g) was treated under dynamic vacuum for 10 min at ambient temperature and suspended in 175 mL anhydrous pyridine and 8 mL 3-aminopropyltriethoxysilane (99%, Sigma-Aldrich), and stirred and heated to reflux under $N_2$ for 24 h. The solids were filtered and washed with toluene, tetrahydrofuran, and dichloromethane (3 × 50 mL), Soxhlet extracted in toluene for 24 h,
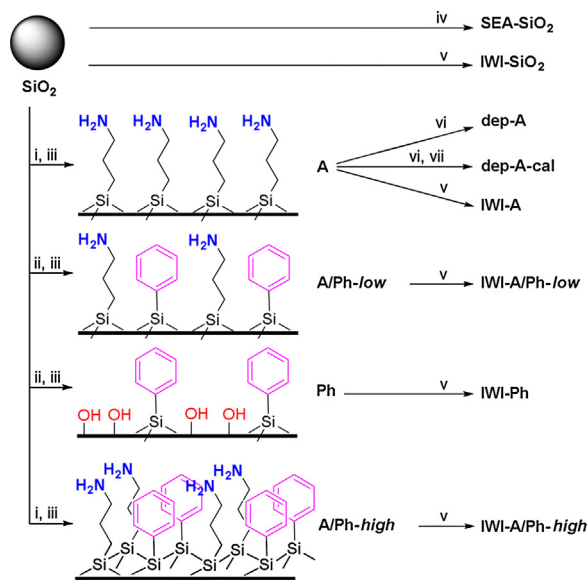


**Scheme 2.** Synthesis of organosilane-modified and control Pd catalysts. For full synthesis details, see text. (i) Dynamic vacuum RT, 1 h; (ii) dynamic vacuum 150 °C, 2 h; (iii) 3-aminopropyl-triethoxysilane and/or phenyl-trimethoxysilane in pyridine, reflux under $N_2$ overnight; (iv) solution pH adjusted with $NH_4OH$, adsorption of tetraamine Pd(II) nitrate (aq), filter, dry, grind; (v) incipient wetness impregnation of Pd(II) acetate from minimum dichloromethane, dry, grind; (vi) reflux with Pd(II) acetate in dichloromethane/toluene, filter, wash, dry, grind; (vii) calcine in air to 350 °C. All catalysts reduced in $H_2$ at 350 °C before catalytic testing.

dried under vacuum at 100 °C, and sieved to 63 μm average particle size.

### 2.3. Phenylsilane-modified silica (**Ph**)

Silica (2 g), was treated under dynamic vacuum at 150 °C for 2 h, suspended in 50 mL pyridine and 1.1 mL of phenyltrimethoxysilane (Gelest Inc.), and heated to reflux for 18 h under $N_2$. The solids were recovered by filtration, and washed with toluene, tetrahydrofuran, and dichloromethane (3 × 25 mL). After overnight Soxhlet extraction in toluene, the materials were dried under vacuum at 100 °C overnight, and sieved to 63 μm average particle size.

### 2.4. Mixed organosilane modification

Silica (2 g) was suspended in 50 mL pyridine, 3-aminopropyltriethoxysilane, and phenyltrimethoxysilane, and refluxed 18 h under $N_2$. The solids were recovered by filtration, and washed with toluene, tetrahydrofuran, and dichloromethane (3 × 25 mL). After overnight Soxhlet extraction in toluene, the materials were dried under vacuum at 100 °C overnight, and sieved to 63 μm average particle size. **A/Ph-*low*** first pretreated the silica under vacuum at 150 °C for 2 h and used 0.55 mL and 0.70 mL 3-aminopropyltriethoxysilane and phenyltrimethoxysilane, respectively (45 mol% 3-aminopropyltriethoxysilane). **A/Ph-*high*** was only dried at room temperature, and used 0.85 mL and 0.43 mL 3-aminopropyltriethoxysilane and phenyltrimethoxysilane, respectively (67 mol% 3-aminopropyltriethoxysilane).

### 2.5. Pd incorporation by incipient wetness impregnation (**IWI**)

Pd acetate was incorporated at 3 wt% loading from dichloromethane. This solvent was chosen to follow previously reported, related procedures [20]. The Pd solution was added dropwise until the minimum wetting volume was reached and the material was undisturbed for 24 h. The material was vacuum dried

overnight and lightly ground to break up aggregates. A family of materials labeled **IWI** were synthesized by this method.

### 2.6. Pd incorporation by strong electrostatic adsorption (**SEA** [22])

Silica (2 g) was slurried with aqueous ammonium hydroxide to reach pH 11. To this, 1.2 mL of tetraaminepalladium (II) nitrate solution (5 wt% Pd in water, Strem Chemicals) was added, the slurry sonicated for 20 min, and left to stand for 20 min. The solids were recovered by filtration, vacuum dried overnight, and lightly ground to break up aggregates to synthesize material **SEA-SiO$_2$**.

### 2.7. Pd incorporation by deposition (**dep**)

Pd acetate (98% min., Strem Chemicals, 133 mg) was dissolved in 5 mL dichloromethane and added to a suspension of 2 g functionalized silica **A** in 50 mL of toluene. The suspension was heated to reflux for 24 h, the solids containing deposited Pd were filtered and washed with 25 mL of toluene and dichloromethane, dried under vacuum for 4 h, and lightly ground to break up aggregates to synthesize material **dep-A**.

### 2.8. Commercial catalysts

Some experiments used commercial **Pd/C** (3 wt% Pd, Sigma-Aldrich) or Pd/SiO$_2$ (**Pd/SiO$_2$**, 5% Pd, reduced, dry, Escat$^{TM}$ 1351, Strem Chemicals) synthesized by unknown methods.

### 2.9. General material characterization

Thermogravimetric analysis was performed on a TA Instruments Q500 instrument. Samples were heated to 800 °C at a ramp rate of 20 °C/min in 90/10 O$_2$/N$_2$. The loading of organics was estimated from the weight loss in the range 200–700 °C. N$_2$ adsorption and desorption isotherms were measured at its normal boiling point using a Micromeritics ASAP 2010. The Brunauer-Emmett-Teller method was used to determine surface area, SA$_{BET}$; maximum pore volumes, V$_{pore}$, were calculated from N$_2$ uptake at P/P$_0$ = 0.99. Pd loadings were calculated for as-made catalyst samples: 30–50 mg of catalyst powder was digested in 1 mL concentrated HF (45–51 wt%) and 1 mL aqua regia (3:1 v/v HCl/HNO$_3$), then diluted with 18 MΩ purified water. CAUTION: handle HF and aqua regia with all appropriate safety precautions. Pd loadings were determined with a Varian Vista-MPX ICP-OES. Carbon and nitrogen contents were determined by Galbraith Laboratories, Inc. by combustion analyses. The surface charge of various catalyst samples was characterized by measurement of their isoelectric points (IEP). Approximately 15 mg of sample was suspended in 15 mL of purified water, sonicated several minutes to break up agglomeration, and the suspension pH was adjusted with NH$_4$OH or HNO$_3$ and measured with a VWR symphony SP70 P pH meter fitted with a calibrated Ag/AgCl electrode after 1 h stabilization. The zeta potential at each pH was measured using a Malvern Instruments Nano ZS Zetasizer at room temperature. The IEP was determined by interpolating the pH where the zeta potential reaches zero. Diffuse Reflectance Infrared Fourier Transform Spectroscopy (DRIFTS) was carried out in a Harrick Praying Mantis cell with ZnSe windows and a Thermo Nicolet 6700 IR spectrometer. 64 scans were acquired for both background and sample spectra at a resolution of 0.96 cm$^{-1}$. $^{13}$C cross-polarized magic angle spinning (CP/MAS) NMR spectra were acquired with a Varian 400 MHz magnet at 10 kHz spinning and 2000–3000 scans.

### 2.10. Pd dispersion

CO pulse chemisorption was carried out with an Altamira AMI-200 instrument. Prior to CO chemisorption, the as-synthesized catalysts were reduced in dilute H$_2$ (10% H$_2$, balance Ar, Matheson Tri-Gas) at 250 °C, then cooled to 30 °C under He (99.999%, Airgas). Dilute CO (5% CO, balance He) was then pulsed to the catalyst bed at 1.33 μmol CO per pulse, allowing 4 min between pulses. The amount of CO in the effluent was measured by a thermal conductivity detector (TCD). CO uptake was calculated from TCD peak areas relative to operation at steady state once the catalyst surface is saturated with chemisorbed CO. Run to run variability for CO uptake was ±2%. Pd dispersion (D$_{Pd}$) assumed a stoichiometry of 1 surface Pd per adsorbed CO. Transmission electron microscopy (TEM) was carried out on a JEOL 2100 microscope at 200 kV. Samples were dropped onto grids from ethanol suspensions.

### 2.11. Catalytic deoxygenation of stearic acid

Before testing, all catalysts were reduced under flow of 30 mL/min of H$_2$ at 350 °C for 15 min after a ramp at 2 °C/min in a 35 mL, in a heavy-wall glass pressure vessel (Chemglass, tube form factor). The catalysts were sealed and immediately transferred to an Ar glovebox, avoiding air exposure. In an Ar glovebox, 0.05 M solutions of stearic acid (Grade I approx. 99%, Sigma-Aldrich) in dodecane (anhydrous, distilled from CaH$_2$) with 1 v/v% tetradecane (distilled from CaH$_2$) as an internal standard were prepared and heated to 45 °C to ensure full dissolution. While in the glovebox, 2 mL solution were added to the pressure vessels typically containing 200 mg of reduced catalyst, and the reactors sealed with a Teflon plug. CAUTION: exercise all appropriate caution with glass pressure vessels. Reactions must be carried out behind a safety shield. The reactors were immersed in an aluminum bead bath and heated for 6 h to 300 °C, measured at the point of contact between the vessel and the bead bath, while shaking the whole apparatus. Catalyst loading for each reaction is given in μmol surface Pd (Pd$_{surf}$) calculated from the product of the mass of catalyst in the reaction, the wt. fraction Pd, and the fractional Pd dispersion, then divided by the molecular mass of Pd.

Following reaction, the reactors were cooled and the contents centrifuged to form a catalyst pellet. While heating the supernatant at 45 °C to ensure full dissolution of stearic acid, 100 μL samples of supernatant were extracted and mixed with 900 μL 0.2 M BSTFA (N,O-bis(trimethylsilyl) trifluoroacetamide, >99.0%, Sigma-Aldrich) in pyridine for derivatization of remaining stearic acid. The samples were sealed and heated to 60 °C for 1 h. Products were identified with a Shimadzu GC-2010 Plus fitted with a Shimadzu QP2010 SE mass spectrometer. Product quantification was carried out in a Shimadzu GC-2010 GC-FID. 3.0 μL samples were injected (250 °C, 50:1 split ratio) into a 30 m × 0.24 mm × 0.25 μm TR-1 column with 3.42 mL/min of He carrier flow. The column was maintained at 100 °C for 10 min and then heated at 5 °C/min to 290 °C for 30 min. FID response factors were developed for BSTFA-derivatized stearic acid and heptadecane relative to the tetradecane internal standard. Heptadecane response factors were applied to all C$_{17}$ products observed, as is reasonable for a FID. Results are reported as total C$_{17}$ yield relative to added stearic acid and the selectivity to *n*-heptadecane as a fraction of all C$_{17}$ products.

## 3. Results and discussion

### 3.1. Unmodified supports

Initial investigations were carried out with Pd supported on unmodified silica prepared by incipient wetness impregnation

**Table 1**
Properties of Pd supported on unmodified $SiO_2$ and carbon.

| Catalyst | Notes | $SA_{BET}$ ($m^2$/g) | $V_{pore}$ ($cm^3$/g) | IEP | wt% Pd | $D_{Pd}$ (%) |
|---|---|---|---|---|---|---|
| $SiO_2$ | Fumed Silica | 340 | 2.3 | 1.0[a] | – | – |
| Pd/C | Pd/C Sigma Aldrich | 1250 | 0.7 | 1.0[a] | 3.0 | 29 |
| $Pd/SiO_2$ | $Pd/SiO_2$ Strem | 290 | 1.2 | 3.0[a] | 5.1 | 4 |
| SEA-$SiO_2$ | $(NH_3)_4Pd(NO_3)_2$ by SEA | 320 | 1.6 | 3.5[b] | 2.7 | 45 |
| IWI-$SiO_2$ | $Pd(Ac)_2$ by IWI | 330 | 1.6 | 5.0[b] | 2.6 | 34 |

[a] As received.
[b] Reduced in $H_2$ at 350 °C prior to measurement.

(**IWI-SiO$_2$**) and strong electrostatic adsorption (**SEA-SiO$_2$**), and their properties are compared to samples of commercial **Pd/SiO$_2$** and **Pd/C** in Table 1. The materials synthesis conditions were chosen to match preparations reported by others in the literature [22,23].

After deposition of Pd by IWI or SEA, the surface area of the silica support is not significantly changed, but there is some change to the inter-particle packing, as indicated by the decrease in pore volume. The residual silica surface is also not dramatically changed, with the IEP of the **IWI-SiO$_2$** and **SEA-SiO$_2$** catalysts remaining in the acidic range. (Supporting information Fig. S1) The commercial **Pd/SiO$_2$** catalyst is of a surface area comparable to the experimental samples and an IEP similar to other silica supported catalysts. Finally, the commercial **Pd/C** catalyst is of markedly higher surface area and has an acidic IEP, indicating an oxidized activated carbon support [24]. This sample is supported on alkali-modified activated carbon, and creates a markedly basic solution, (pH = 9.4 from 100 mg catalyst dispersed in 0.5 mL $H_2O$) presumably from desorption of the alkali countercations and other inorganics when in water.

Pd loadings are all ~2.7–2.9 wt% on the experimental samples, **SEA-SiO$_2$** and **IWI-SiO$_2$**, to match the loading on **Pd/C**. All experimental samples have dispersions of 33–45%, indicating supported nanoparticles. The commercial **Pd/SiO$_2$** has a higher loading but very poor dispersion. Overall, while the high surface area of the carbon support undoubtedly helps maintain the Pd dispersion, silica supports are also readily decorated with small Pd nanoparticles.

### 3.2. Stearic acid deoxygenation by Pd on unmodified supports

These Pd-containing catalysts were then examined in the deoxygenation of stearic acid under Ar at 300 °C for 6 h, with results shown in Table 2. Stearic acid conversion approached 100% in nearly all cases, not necessarily with corresponding yields of heptadecane or other seventeen-carbon ($C_{17}$) species, resulting in poor mass balances. This is attributed to the known strong adsorption of stearic acid onto silica [25], which we also observed. As shown in Supporting information Fig. S2, a used catalyst with an unmodified support can easily retain (adsorb or strongly include in the pore volume) more than 30% of all the originally added stearic acid at the catalytic conditions used, which accounts for the majority of the incomplete mass balance. This is partially a consequence of the relatively low substrate:catalyst ratios used in order to rapidly

**Table 2**
Catalytic deoxygenation screening results for Pd/C and Pd on unmodified silica supports.

| Catalyst | Catalyst (mg) | $Pd_{surface}$ (μmol)[a] | $C_{17}$ yield | Selectivity[b] |
|---|---|---|---|---|
| $Pd/SiO_2$ | 200 | 4 | 0 | – |
| Pd/C | 200 | 16 | 73 | 99 |
|  | 50 | 4 | 70 | 63 |
| SEA-$SiO_2$ | 200 | 23 | 38 | 74 |
|  | 90 | 10 | 13 | 49 |
| IWI-$SiO_2$ | 200 | 19 | 4 | 51 |

[a] See Section 2.11 for definition.
[b] Selectivity to n-heptadecane. All significant other products are positional isomers of heptadecene. See chromatogram in Supporting information Fig. S3.

differentiate the sample preparations and may not be as significant under optimized reactor loadings. The small volumes used in this screening study, and the significant accumulation of solidified reactants inside the catalyst pores, precluded studies of catalyst recycling.

Due to these losses from adsorption, catalytic activity was compared in terms of $C_{17}$ yield, not conversion (disappearance of stearic acid reactant). Products appeared as a succession of closely-spaced peaks in the chromatogram (Supporting information Fig. S3) and were identified by mass spectrometry as various $C_{17}$ species. In addition to the desired n-heptadecane, the principal remaining products were positional isomers of heptadecene. Small amounts (<1%) of $C_{17}$ alkyl aromatics were detected in some of the catalysts with highest total n-heptadecane selectivity. Small amounts of heavy esters were also indicated in all reactions, including in the absence of added catalyst, presumably produced by stearic acid reacting with alcohol impurities present in the reaction mixture.

Higher selectivity correlated with higher yield, reaching almost complete selectivity at full conversion (see Supporting information Fig. S4). This is consistent with previously proposed reaction pathways by which decarboxylation/decarbonylation to n-heptadecane and n-heptadecene occur in parallel at low to intermediate conversions, followed by hydrogenation of any unsaturated product by hydrogen transfer from the dodecane solvent, to result in a final saturated product [12].

Table 2 collects the results of stearic acid deoxygenation over Pd on unmodified $SiO_2$ catalysts and the control **Pd/C** catalyst. Of all catalysts tested, **Pd/C** displayed the best yield and selectivity even at lowered catalyst loadings, and superior to all of the unmodified silica-supported catalysts, in agreement with previous observations [18]. Despite having the highest metal loading, commercial **Pd/SiO$_2$** performs very poorly, failing to generate any detectable product, which can be attributed to its very poor Pd availability.

Experimentally prepared samples using SEA or IWI faired significantly better than the commercial silica catalyst, again, presumably due to increased Pd availability. The data for catalysts that were tested at two different loadings (**Pd/C** and **SEA-SiO$_2$** in Table 2) show that n-heptadecane yields increased with surface Pd available in the reactor, as expected. However, despite all silica-supported catalysts having better Pd dispersion than **Pd/C**, they were unable to achieve its productivity, even when decreasing the **Pd/C** loading by 75%. Further, **SEA-SiO$_2$** outperforms **IWI-SiO$_2$**, even when loadings are halved. Amongst the supported catalysts in Tables 1 and 2, neither Pd dispersion nor active Pd loading alone are able to predict product yields, and unmodified silica seems to be a far worse support than activated carbon. Thus, surface effects due to the support and preparation method appear to be significant.

### 3.3. Organosilane-modified supports

Previously, researchers have succeeded in preparing highly active **Pd/SiO$_2$** catalysts for stearic acid deoxygenation by first depositing Pd precursors onto an amine-modified mesoporous silica, followed by treatment in $O_2$, then catalyst reduction [20]. Here

**Table 3**
Summary of physical properties of organosilane modified silica support materials.

| Support | Total organics[a] | | Amines | SA$_{BET}$ | V$_{pore}$[c] | IEP |
|---|---|---|---|---|---|---|
| | grafts/nm$^2$ | mmol/g | (mmol/g) | (m$^2$/g) | (cm$^3$/g) | |
| Ac. Carbon[d] | – | – | – | 1250 | 0.7 | 1.0 |
| SiO$_2$ | – | – | – | 340 | 2.3 | 1.0 |
| A | 2.3 | 1.3 | 1.3 | 210[b] | 1.8 | 9.5 |
| Ph | 0.8 | 0.4 | 0 | 320[b] | 1.8 | 3.0 |
| A/Ph-*low* | 2.7 | 1.5 | 0.8 | 240[b] | 1.9 | 8.5 |
| A/Ph-*high* | 9.6 | 5.4 | 0.9 | 220[b] | 1.2 | 9.0 |

[a] Calculated from combustion analysis by TGA and normalized to BET surface areas.
[b] Per g unmodified SiO$_2$.
[c] Calculated at P/P$_0$ = 0.99.
[d] Properties taken from the commercial Pd/C sample.

we seek to understand whether the role of similar silane modifications are primarily to alter Pd availability, or if other support properties such as basicity and hydrophobicity also play a role. Organosilane modifiers were 3-aminopropylsilane and phenylsilane, to add basic and aromatic functionality respectively. These modifiers were chosen to follow up on prior reports and potentially to mimic the reaction environment generated by alkaline activated carbons [7,26].

The properties of unmodified silica and four silane-grafted silica supports are reported in Table 3. In most cases, organosilanes were deposited under anhydrous conditions and drying of the silica sample beforehand to limit silane deposition to (sub) monolayer coverage. For these supports, total silane loadings range from 0.8 to 2.3 grafts/nm$^2$ (0.4 to 1.3 mmol/g). Materials **A** and **Ph** consist of silica functionalized with 3-aminopropyl and phenyl groups respectively, and were prepared to investigate how these functional groups independently affected catalyst activity. The other two materials, **A/Ph-*low*** and **A/Ph-*high*** were prepared as a mixture of these two functional groups. By combustion CHN analysis, **A/Ph-*low*** contains ~0.8 mmol/g amines and a similar loading of phenyl groups. For **A/Ph-*high***, the mixed silanes were grafted without aggressive drying to give some vertical polymerization of the organosilanes. This ratio of the two organosilanes gave a similar amine loading of ~0.9 mmol/g, but a much higher phenyl loading of ~4.5 mmol/g. The total surface density of ~9.6 grafts per nm$^2$ is in excess of typical silanol numbers on silica [27] and reflects a dense layer completely covering the original surface. $^{13}$C CP/MAS NMR shows both the phenyl and propylamine surface groups (Supporting information Fig. S5). Likewise, DRIFTS shows aliphatic C—H stretches (propyl amine) near 2900 cm$^{-1}$ and a weaker C—H stretch near 3050 cm$^{-1}$ assigned to the phenylsilane (Supporting information Fig. S6).

Surface areas for all silica-based materials, including unmodified silica, are 210–340 m$^2$/g (see Supporting information Fig. S7), facilitating comparisons. Increasing loadings of organosilanes generally decreased available surface areas and pore volumes from the parent SiO$_2$ material. The porosity in these fumed silica materials arises from mesoporosity formed by aggregation of the primary, non-porous particles; surface functionalization can disrupt this aggregation, decreasing the pore volume and surface area, in some cases significantly. In contrast, the commercial carbon sample is largely microporous and has a very high surface area but a small pore volume.

The isoelectric point (IEP) of the supports was measured as a probe for the relative acidity/basicity of the surfaces (Supporting information Fig. S1). As expected, **A** has the most basic IEP owing to the high loading of basic amine groups on its surface. As already noted, the particular activated carbon support in the commercial **Pd/C** has an acidic IEP, but generates a basic environment due to alkali exchange onto the oxidized surface. In contrast, **Ph** has a low
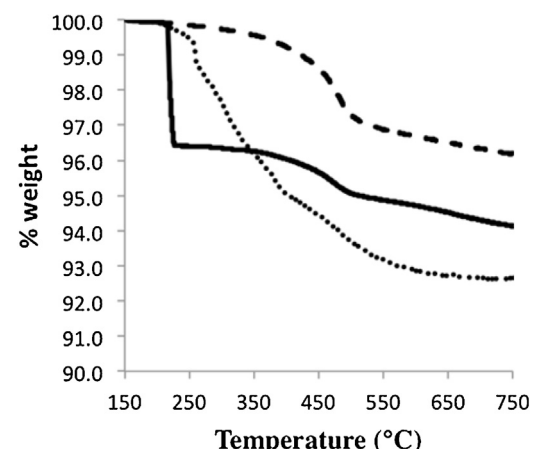


**Fig. 1.** Thermogravimetric analysis comparing **A** (dotted) with **dep-A** (solid) and **dep-A-*cal*** (dashed). Organic contents increase in the order **dep-A-*calc*** < **dep-A** < **A**.

IEP comparable to the SiO$_2$ parent support. Its relatively low grafting density allows residual surface silanols to contribute to surface acidity. The mixed organosilane materials **A/Ph-*low*** and **A/Ph-*high*** also have basic IEPs largely indistinguishable from **A**, due to the 3-aminopropyl groups they share in common.

Pd was incorporated onto these modified silica supports from Pd acetate either by deposition (**dep**) from dichloromethane/toluene following prior procedures [20,28], or by incipient wetness impregnation (**IWI**), also from dichloromethane. The materials are referred to by their incorporation method followed by the support name; for example, **IWI-A** refers to a catalyst that was prepared by incipient wetness impregnation of support **A**. In most cases, the catalyst was immediately reduced after Pd incorporation, but in one case, the catalyst sample was first calcined in air at 350 °C before reduction (**dep-A-*cal***).

The physical properties of the resulting catalysts are given in Table 4. Incorporation of Pd does not generally alter the physical properties of the catalyst in a significant way, except for the aminopropylsilane-modified support **A**, where the heat treatments following Pd incorporation restore much of the original surface area of the parent SiO$_2$ surface, indicating a significant change in surface properties. Thermogravimetric analysis (TGA), Fig. 1, after the reductive heat treatment for **dep-A** shows only 22% less mass loss as compared to the patent support **A**, while TGA after the oxidative treatment for **dep-A-*cal*** shows 50% less mass loss. These results give evidence of only partial removal of the amine groups by the reductive pretreatment, and significant loss of the organic surface functionality during calcination then reduction. Moreover, removal of amine groups during calcination prior to reduction results in an IEP of ~4 for **dep-A-*calc*** as opposed to ~9 for **dep-A**, consistent with significant loss of the amine groups for **dep-A-*calc*** and only partial loss and/or a restructuring of the amines for **dep-A**. The IEP also shows a significant drop after Pd incorporation for **IWI-A/Ph-*low***, consistent with a loss of free amine groups via coordination to Pd. However, there are few changes otherwise, which is consistent with the absence of significant changes in the $^{13}$C CP/MAS NMR and DRIFTS (Supporting information Figs. S5 and S6) when the mixed organosilane material **A/Ph-*low*** is treated in H$_2$ at 350 °C to mimic pretreatment conditions.

Pd dispersions on the organosilane-modified surfaces are uniformly high, exceeding those of the commercial **Pd/C** catalyst. TEM of the IWI-synthesized catalysts is consistent with the high dispersion, showing predominately small nanoparticles <2 nm, and none of the larger clusters seen with **Pd/C** (8.5 ± 5.6 nm) or **SEA-SiO$_2$** (4.5 ± 1.7 nm) both of which are already quite well dispersed. (Supporting information Fig. S8.) All of the aminopropylsilane-grafted

**Table 4**
Properties of Pd supported on organosilane-modified silica.

| Catalyst | $SA_{BET}$[a] $(m^2/g)$ | $V_{pore}$[b] $(cm^3/g)$ | IEP | wt% Pd | $D_{Pd}$ (%) | size (nm)[c] |
|---|---|---|---|---|---|---|
| dep-A | 280 | 1.9 | 9.0 | 2.2 | 45 | |
| dep-A-*cal* | 310 | 1.7 | 4.0 | 1.6 | 37 | |
| IWI-A | 300 | 1.5 | 10.0 | 1.9 | 46 | 1.4 |
| IWI-Ph | 320 | 1.8 | 3.0 | 3.1 | 35 | 2.1 |
| IWI-A/Ph-*low* | 250 | 1.7 | 4.5 | 2.2 | 55 | 1.5 |
| IWI-A/Ph-*high* | 190 | 0.9 | 8.0 | 3.0 | 35 | 1.7 |

[a] Per g $SiO_2$. Physisorption carried out after reduction.
[b] Calculated at $P/P_0 = 0.99$.
[c] Average particle size +/−0.5 nm by TEM.

materials contain more amine groups than incorporated Pd, which may partially explain the good dispersions achieved. In addition to altering the surface charge, calcination prior to reduction in **dep-A-*cal*** also aggregates the Pd nanoparticles resulting in lower dispersion, and some Pd is lost to the calcination vessel. This may indicate that the Pd is weakly attached to the amine grafts, rather than to the silica surface, and becomes mobile during calcination.

### 3.4. Deoxygenation results

The catalysts of Table 4 were then used in the deoxygenation of stearic acid (Table 5). With the exception of **dep-A-*cal***, all the organosilane-modified catalysts had similar moles of surface Pd in the reactor, meaning that differences in the activity cannot be attributed to differences in loading. Table 4 showed that all catalysts have similar dispersions as well, controlling for any structure-sensitivity of the reaction on the Pd surface itself. Grafting organosilanes onto **SEA-SiO$_2$**, i.e. after Pd incorporation, gives poor or inactive catalysts (Supporting information Section 9), demonstrating that, as expected, the Pd surface itself must not be blocked for catalysis to occur. **dep-A** showed markedly higher $C_{17}$ yields than any of the unmodified silica-supported catalysts (Table 2), and gave the high selectivity of **Pd/C**. Likewise, IWI of Pd on the same support (**IWI-A**), gives a catalyst with very similar performance, confirming that the surface modifiers, and not the method of Pd incorporation, primarily determine the changes in reactivity. In contrast, **dep-A-*cal*** was prepared by calcination prior to reduction, as in the previous work using this catalyst preparation [20], removing organic groups from the support. While there is less surface Pd in the reactor for **dep-A-*cal*** than **dep-A**, performance in terms of yield drops more significantly, to a level comparable to that of Pd on unmodified silica, such as a sample of **SEA-SiO$_2$** with similar Pd availability. This again indicates that the increased performance of the **dep-A** catalyst, as compared to the unmodified supports, is not related to Pd dispersion or total available surface Pd alone, but is also a consequence of the support properties, implicating catalysis at interface sites.

Roles of the organic modifying groups include titrating surface silanols or affecting the surface charge and polarity. Researchers have previously observed that catalyst surface charge and polarity have effects on catalyst performance for deoxygenation of stearic acid and its esters, with basic supports being favorable [7,8,10,21,29]. Moreover, carboxylic acids are known to react irreversibly with silanols to form esters at the temperatures necessary for this reaction [30,31]. Therefore, additional materials were investigated to further modify surface basicity and polarity.

First, a portion of the surface silanols were capped with phenylsilane (**IWI-Ph**). The activity of **IWI-Ph** is not markedly improved relative to the unmodified silica supports and **dep-A-*cal***. With the presence of both aromatic rings and residual oxygen defects (free silanols, in this case), **IWI-Ph** mimics somewhat the structure of carbon surfaces, and demonstrates that for these materials, the residual oxygen defect are problematic unless completely titrated away. For this reason, **IWI-Ph** is inferior to either **IWI-A** or **dep-A**, and markedly underperforms relative to **Pd/C**.

Next, amine sites and phenylsilanes were combined in **IWI-A/Ph-*low*** and **IWI-A/Ph-*high***, resulting in dramatically improved yield and *n*-heptadecane selectivity. The improvement for these combined catalysts parallels the known enhancement of activity in alkaline-modified [7,8,10] and more polar [21] carbon supports. It is suggested that the basic aminopropyl-modified surface may provide adsorption sites of the appropriate strength and geometry to orient the carboxylic acid moiety in stearic acid at the Pd-support interface [32], while the co-grafted phenylsilane may prevent product deactivation and coking on the residual oxide surface. Regardless of mechanism, this synergy between the phenyl and aminopropyl groups becomes clear when noting that **IWI-A/Ph-*low*** results in better yields than **IWI-A** despite similar organic loadings in mixed material. The optimal yields are achieved over **IWI-A/Ph-*high***, which exceeds that of the **Pd/C** reference and gives greater than 85% yield of *n*-heptadecane. The synthesis method for this catalyst leads to vertical polymerization of the silanes, completely isolating the Pd particles from the original silica surface. All three roles of the organosilane modifier – decreasing silanols and controlling surface charge and polarity – culminate in the performance of **IWI-A/Ph-*high***.

While there has been much work in designing hybrid organic-inorganic materials for catalysis, research has mostly focused on immobilizing effective homogenous catalysts onto a support [33–35], and not in fine-tuning the surface properties of the support when the catalytic species are metal nanoparticles. An example of this latter focus is a report by Sari et al. in which activated carbon was modified with silica prior to Pd incorporation and resulted in good catalysts for free fatty acid decarboxylation [36]. Moreover, recent reports have demonstrated the importance of tuning the microenvironment on the support surface for enhancement of heterogeneous catalysis [37–40]. For example, Wang and co-workers found that using a superhydrophobic silica support enhanced the catalytic activity of Pt for alcohol oxidation because of improved

**Table 5**
Catalytic deoxygenation results for catalysts prepared on organic modified silica.

| Support | Catalyst (mg) | $Pd_{surf}$ ($\mu$mol)[a] | $C_{17}$ yield | Selectivity[b] |
|---|---|---|---|---|
| SEA-SiO$_2$[c] | 90 | 10 | 13 | 49 |
| dep-A-*cal* | 200 | 11 | 14 | 43 |
| dep-A | 200 | 19 | 51 | 100 |
| IWI-A | 200 | 17 | 62 | 96 |
| IWI-Ph | 200 | 21 | 20 | 48 |
| IWI-A/Ph-*low* | 200 | 23 | 70 | 95 |
| IWI-A/Ph-*high* | 200 | 21 | 93 | 93 |

[a] See Section 2.11 for definition.
[b] Selectivity to *n*-heptadecane. All significant other products are positional isomers of heptadecene. See chromatogram in Supporting information Fig. S3.
[c] Repetition of results in Table 3 for clarity.

mass transfer of aliphatic alcohols onto the catalyst surface and exclusion of polar byproducts [38]. In another example, silica modified with phenyl groups performed better than silica modified with methyl groups or bare silica as supports for Pd nanoparticles in Heck coupling reactions, illustrating the importance of tuning the polarity/polarizability of the support in improving catalyst performance [39]. Finally, Kandel et al. recently demonstrated that 3-aminopropyl groups on silica can improve free fatty acid decarboxylation catalyzed by supported Ni [32], rather than rapid deactivation on bare silica, similar to our findings. Our combination of basic sites embedded in the polarizable phenylsilane layer in **IWI-A/Ph-*high*** appears to further optimize the adsorption of stearic acid and may act by limiting product poisoning or coking.

## 4. Conclusions

Overall, the examination of a range of Pd catalysts incorporated by different methods onto silica and organosilane-modified silica provided new insights into the role of the support in the catalytic deoxygenation of stearic acid. Bare silica is a poor support, even when Pd dispersions are similar to those on the high-performing Pd/C catalyst. However, modifying the silica support with mixtures of basic aminopropylsilane and polarizable phenylsilanes allows us to mimic some of the surface properties of activated carbon that are important for maintaining yields, ultimately giving a catalyst with greatly improved performance.

While activated carbons remain a viable support for this reaction due to their low cost and their own options for tuning the surface properties, the organosilane-modified materials in this paper illustrate the potential and importance of fine tuning surface properties for oxide-supported metal nanoparticle catalysts using organosilanes. Organosilane modification applied to supported nanoparticles has seen much less attention than similar modifications for immobilized homogeneous catalysts or for oxide catalysts. Such hybrid supports can be designed to combine the robustness and porosity of inorganic supports, while independently tuning their surface properties to optimize reactant and product adsorption, which may help improve catalyst longevity or ease of regeneration. The latter are important topics when a reaction moves towards commercialization, and in particular, this may lead to improvements in challenging reactions such as biomass deoxygenation for the renewable production of green diesel, as studied here. Any future studies will directly address the challenge of catalyst recycling and reaction optimization for these hybrid supports.

## Acknowledgments

## Appendix A. Supplementary data

Supplementary data associated with this article can be found, in the online version, at http://dx.doi.org/10.1016/j.apcatb.2016.03.041.

## References

[1] Summary for Policymakers, in: O. Edenhofer, R. Pichs-Madruga, Y. Sokona, K. Seyboth, P. Matschoss, S. Kadner, T. Zwickel, P. Eickemeier, G. Hansen, S. Schlömer, C. von Stechow (Eds.), IPCC Special Report on Renewable Energy Sources and Climate Change Mitigation, Cambridge University Press Cambridge, United Kingdom and New York, NY, USA, 2011.

[2] G.W. Huber, S. Iborra, A. Corma, Synthesis of transportation fuels from biomass: chemistry, catalysts, and engineering, Chem. Rev. 106 (2006) 4044–4098.

[3] G.W. Huber, P. O'Connor, A. Corma, Processing biomass in conventional oil refineries: production of high quality diesel by hydrotreating vegetable oils in heavy vacuum oil mixtures, Appl. Catal. A: Gen. 329 (2007) 120–129.

[4] T.A. Foglia, P.A. Barr, Decarbonylation dehydration of fatty acids to alkenes in the presence of transition metal complexes, J. Am. Oil Chem. Soc. 53 (1976) 737–741.

[5] E. Santillan-Jimenez, M. Crocker, Catalytic deoxygenation of fatty acids and their derivatives to hydrocarbon fuels via decarboxylation/decarbonylation, J. Chem. Technol. Biotechnol. 87 (2012) 1041–1050.

[6] I. Kubičková, M. Snåre, K. Eränen, P. Mäki-Arvela, D.Y. Murzin, Hydrocarbons for diesel fuel via decarboxylation of vegetable oils, Catal. Today 106 (2005) 197–200.

[7] M. Snåre, I. Kubičková, P. Mäki-Arvela, K. Eränen, D.Y. Murzin, Heterogeneous catalytic deoxygenation of stearic acid for production of biodiesel, Ind. Eng. Chem. Res. 45 (2006) 5708–5715.

[8] S. Lestari, I. Simakova, A. Tokarev, P. Mäki-Arvela, K. Eränen, D. Murzin, Synthesis of biodiesel via deoxygenation of stearic acid over supported Pd/C catalyst, Catal. Lett. 122 (2008) 247–251.

[9] M. Snåre, I. Kubičková, P. Mäki-Arvela, D. Chichova, K. Eränen, D.Y. Murzin, Catalytic deoxygenation of unsaturated renewable feedstocks for production of diesel fuel hydrocarbons, Fuel 87 (2008) 933–945.

[10] P. Mäki-Arvela, I. Kubickova, M. Snåre, K. Eränen, D.Y. Murzin, Catalytic deoxygenation of fatty acids and their derivatives, Energy Fuels 21 (2007) 30–41.

[11] P. Mäki-Arvela, M. Snåre, K. Eränen, J. Myllyoja, D.Y. Murzin, Continuous decarboxylation of lauric acid over Pd/C catalyst, Fuel 87 (2008) 3543–3549.

[12] J.G. Immer, M.J. Kelly, H.H. Lamb, Catalytic reaction pathways in liquid-phase deoxygenation of C18 free fatty acids, Appl. Catal. A: Gen. 375 (2010) 134–139.

[13] A.S. Berenblyum, T.A. Podoplelova, R.S. Shamsiev, E.A. Katsman, V.Y. Danyushevsky, On the mechanism of catalytic conversion of fatty acids into hydrocarbons in the presence of palladium catalysts on alumina, Pet. Chem. 51 (2011) 336–341.

[14] A.T. Madsen, B. Rozmysłowicz, I.L. Simakova, T. Kilpiö, A.-R. Leino, K.N. Kordaś, K. Eränen, P.I. Mäki-Arvela, D.Y. Murzin, Step changes and deactivation behavior in the continuous decarboxylation of stearic acid, Ind. Eng. Chem. Res. 50 (2011) 11049–11058.

[15] E.W. Ping, J. Pierson, R. Wallace, J.T. Miller, T.F. Fuller, C.W. Jones, On the nature of the deactivation of supported palladium nanoparticle catalysts in the decarboxylation of fatty acids, Appl. Catal. A: Gen. 396 (2011) 85–90.

[16] A. Madsen, B. Rozmysłowicz, P. Mäki-Arvela, I. Simakova, K. Eränen, D. Murzin, R. Fehrmann, Deactivation in continuous deoxygenation of C18-fatty feedstock over Pd/Sibunit, Top. Catal. 56 (2013) 714–724.

[17] I. Simakova, O. Simakova, P. Mäki-Arvela, A. Simakov, M. Estrada, D.Y. Murzin, Deoxygenation of palmitic and stearic acid over supported Pd catalysts: effect of metal dispersion, Appl. Catal. A: Gen. 355 (2009) 100–108.

[18] J. Ford, J. Immer, H.H. Lamb, Palladium catalysts for fatty acid deoxygenation: influence of the support and fatty acid chain length on decarboxylation kinetics, Top. Catal. 55 (2012) 175–184.

[19] S. Lestari, P. Mäki-Arvela, K. Eränen, J. Beltramini, G.Q. Max Lu, D.Y. Murzin, Diesel-like hydrocarbons from catalytic deoxygenation of stearic acid over supported Pd nanoparticles on SBA-15Catalysts, Catal. Lett. 134 (2010) 250–257.

[20] E.W. Ping, R. Wallace, J. Pierson, T.F. Fuller, C.W. Jones, Highly dispersed palladium nanoparticles on ultra-porous silica mesocellular foam for the catalytic decarboxylation of stearic acid, Microporous Mesoporous Mater. 132 (2010) 174–180.

[21] R.W. Gosselink, W. Xia, M. Muhler, K.P. de Jong, J.H. Bitter, Enhancing the activity of Pd on carbon nanofibers for deoxygenation of amphiphilic fatty acid molecules through support polarity, ACS Catal. 3 (2013) 2397–2402.

[22] L. Jiao, J.R. Regalbuto, The synthesis of highly dispersed noble and base metals on silica via strong electrostatic adsorption: I. Amorphous silica, J. Catal. 260 (2008) 329–341.

[23] J. Regalbuto, Catalyst Preparation: Science and Engineering, Taylor & Francis, Boca Raton, FL, 2006.

[24] L.R. Radovic, I.F. Silva, J.I. Ume, J.A. Menéndez, C.A.L.Y. Leon, A.W. Scaroni, An experimental and theoretical study of the adsorption of aromatics possessing

electron-withdrawing and electron-donating functional groups by chemically modified activated carbons, Carbon 35 (1997) 1339–1348.

[25] M. Hasegawa, M.J.D. Low, Infrared study of adsorption in situ at the liquid-solid interface: III. Adsorption of stearic acid on silica and on alumina, and of decanoic acid on magnesia, J. Colloid Interface Sci. 30 (1969) 378–386.

[26] M.L. Toebes, J.A. van Dillen, K.P. de Jong, Synthesis of supported palladium catalysts, J. Mol. Catal. A: Chem. 173 (2001) 75–98.

[27] S. Ek, A. Root, M. Peussa, L. Niinistö, Determination of the hydroxyl group content in silica by thermogravimetry and a comparison with 1H MAS NMR results, Thermochim. Acta 379 (2001) 201–212.

[28] R.B. Bedford, U.G. Singh, R.I. Walton, R.T. Williams, S.A. Davis, Nanoparticulate palladium supported by covalently modified Silicas: Synthesis, characterization, and application as catalysts for the suzuki coupling of aryl halides, Chem. Mater. 17 (2005) 701–707.

[29] M. Watanabe, T. Iida, H. Inomata, Decomposition of a long chain saturated fatty acid with some additives in hot compressed water, Energy Convers. Manage. 47 (2006) 3344–3350.

[30] R.P. Young, Infrared spectroscopic studies of adsorption and catalysis. Part 3. Carboxylic acids and their derivatives adsorbed on silica, Can. J. Chem. 47 (1969) 2237–2247.

[31] K. Marshall, C.H. Rochester, Infrared study of the adsorption of oleic and linolenic acids onto the surface of silica immersed in carbon tetrachloride, J. Chem. Soc. Faraday Trans. 1 71 (1975) 1754–1761.

[32] K. Kandel, C. Frederickson, E.A. Smith, Y.-J. Lee, I.I. Slowing, Bifunctional adsorbent-catalytic nanoparticles for the refining of renewable feedstocks, ACS Catal. 3 (2013) 2750–2758.

[33] A.P. Wight, M.E. Davis, Design and preparation of organic-inorganic hybrid catalysts, Chem. Rev. 102 (2002) 3589–3614.

[34] F. Hoffmann, M. Cornelius, J. Morell, M. Fröba, Silica-Based mesoporous organic–inorganic hybrid materials, Angew. Chem. Int. Ed. 45 (2006) 3216–3251.

[35] J.H. Clark, D.J. Macquarrie, Catalysis of liquid phase organic reactions using chemically modified mesoporous inorganic solids, Chem. Commun. (1998) 853–860.

[36] E. Sari, M. Kim, S.O. Salley, K.Y.S. Ng, A highly active nanocomposite silica-carbon supported palladium catalyst for decarboxylation of free fatty acids for green diesel production: correlation of activity and catalyst properties, Appl. Catal. A: Gen. 467 (2013) 261–269.

[37] C. Chen, J. Xu, Q. Zhang, Y. Ma, L. Zhou, M. Wang, Superhydrophobic materials as efficient catalysts for hydrocarbon selective oxidation, Chem. Commun. 47 (2011) 1336–1338.

[38] M. Wang, F. Wang, J. Ma, C. Chen, S. Shi, J. Xu, Insights into support wettability in tuning catalytic performance in the oxidation of aliphatic alcohols to acids, Chem. Commun. 49 (2013) 6623–6625.

[39] A. Molnar, A. Papp, K. Miklos, P. Forgo, Organically modified Pd-silica catalysts applied in Heck coupling, Chem. Commun. (2003) 2626–2627.

[40] A. Salameh, A. Baudouin, J.-M. Basset, C. Copéret, Tuning the selectivity of alumina-supported $(CH_3)ReO_3$ by modifying the surface properties of the support, Angew. Chem. Int. Ed. 47 (2008) 2117–2120.